THE ASTROPHYSICAL JOURNAL, 345:346–355, 1989 October 1

THE OPTICAL COUNTERPART OF THE X-RAY SOURCE H0253+193: A DISTANT, HIGH-LUMINOSITY RS CANUM VENATICORUM SYSTEM

DAN P. CLEMENS
Department of Astronomy, Boston University

AND

ROBERT W. LEACH
Department of Astronomy, San Diego State University
Received 1988 November 16; accepted 1989 March 15

ABSTRACT

We have detected the optical counterpart of the X-ray source H0253+193 discovered by Halpern and Patterson along the direction toward the nearest molecular cloud L1547 (=MBM 12; distance ~65 pc). Our optical and near-IR photometry in *VRIJHK* and CO (2.35 μm) bands and optical spectroscopy and polarimetry indicate that the optical counterpart is a distant G0–K0 star (distance >200 pc), most likely in a RS CVn binary system. Millimeter-wavelength CO spectroscopic mapping and co-added *IRAS* far-infrared maps indicate moderate extinction through L1547, with lower and upper *V*-band extinction limits of 2.7 and 5 mag, respectively. However, the optical and near-IR colors indicate a visual extinction of 11.3 mag to the star, with an IR-excess possibly due to a cooler binary companion or circumstellar material. The *I*-band polarization of 8.1% ± 1.8% is likely induced in the starlight by passage through the molecular cloud and not due to an embedded reflection nebula. The lack of strong Hα emission in the optical spectrum argues against a classical T Tauri star, while the IR-excess argues against a naked T Tauri star. The high ratio of X-ray to optical flux [log $(F_X/F_V) \sim -1.5$], high X-ray spectral temperature [log $(T) \sim 8.1$], and high X-ray luminosity [log $(L_X) \geq 32$ ergs s^{-1}] are all naturally explained by the RS CVn interpretation. The wide energy spectrum derived from the dereddened optical and near-IR photometry may also favor a binary star model, possibly a G0 V–IV + M5 III pair.

Subject headings: nebulae: individual (L1547) — stars: binaries — stars: individual (H0253+193) — X-rays: sources

I. INTRODUCTION

Studies of the interaction of young T Tauri stars with their molecular environments have revealed much about how low-mass stars form and evolve. Most of these studies have been of the T Tauri stars in well-known, nearby regions of star formation, especially in Taurus-Auriga (Walter *et al.* 1989), upper Scorpius, and in Orion. However, these regions are all greater than 100 pc away.

Halpern and Patterson (1987; hereafter HP) reported finding a hard X-ray source (H0253+193) in the direction of the large, high-latitude and, presumably, nearby molecular cloud L1547. Hobbs, Blitz, and Magnani (1986) and Hobbs *et al.* (1988) used the depth of the sodium absorption lines seen in the optical spectra of stars near the larger, surrounding cloud MBM 12 (Magnani, Blitz, and Mundy 1985) to establish a distance of 65 pc for the molecular system. The X-ray position of the HP object was very near the CO emission center of the MBM 12 cloud, leading HP to conclude that the X-rays were coming from the chromosphere of a T Tauri star embedded in the molecular cloud. No optical counterpart appears on the Palomar Observatory Sky Survey plates at the X-ray position, implying that the extinction to the object must be substantial.

Using the 61 inch (1.5 m) Steward Observatory telescope on Mount Bigelow and our CCD-based imaging polarimeter with a 5′ × 5′ field of view (Clemens and Leach 1987), we searched for faint objects near the X-ray position. We found only one source in the field, and (initially) only in an *I*-band (9000 Å) frame. This object is within 70″ of the X-ray position, only mildly outside of the X-ray error box, and is extremely red. We identify this object as the optical counterpart of H0253+193.

We have subsequently studied this object and the intervening molecular cloud L1457 (MBM 12) using deep optical imaging, optical spectroscopy, near-infrared imaging, far-infrared (*IRAS*) imaging, and millimeter-wave CO spectroscopy. The overall picture of the X-ray source and molecular cloud system which we have developed is somewhat different from the embedded T Tauri star model proposed by HP. We have determined the spectral type of the star to be roughly G5 (perhaps as early as G0, or as late as K0). The star does exhibit a mild infrared excess, one of the characteristics of a classical T Tauri star, though there is no strong Hα emission or absorption in the optical spectrum. The extinction to the star, determined from the optical and near-IR photometry, is about 11.3 mag at *V*-band, which for a star at least as luminous as a main-sequence dwarf, establishes a minimum distance of 200 pc. Thus, the star is far behind the cloud, and not embedded within it. Millimeter CO spectroscopy and *IRAS* co-added imagery yield smaller inferred extinctions through the cloud and show no localized warming or embedded far-infrared sources. A consistent interpretation of the observations from X-ray to millimeter wavelengths favors an RS CVn binary system of high luminosity some 500 pc away, shining (barely) through the nearby molecular cloud.

In the following section, we present our observations of the star and molecular cloud. In § III, the optical spectroscopy and near-IR photometry are combined to obtain a spectral type of

G5 for the star. In § IV, we interpret the observations to show that the extinction to the star, 11.3 mag in the V band, is about the same as that required to explain the hardness of the X-ray spectrum (>10 mag). In § V, the details of the identification of H0253+193 with the I-band star are given. In § VI, we use the interpretation of H0253+193 as an RS CVn binary system to explain the X-ray properties measured by HP. Section VII attempts to explain the width of the broad-band energy distribution obtained from the dereddened optical and near-IR photometry as two stars of dissimilar spectral types and luminosity classes, discussing the details of numerical experiments using binary systems consisting of G0 V–IV + M5 III stars.

II. OBSERVATIONS

We observed the line of sight toward H0253+193 at a variety of wavelengths, from 1.3 mm to 5500 Å, and using a variety of techniques, including deep imaging, spectroscopy, and polarimetry. The observations can be separated into data pertaining to the stellar object found ($\lambda < 10$ μm) and data pertaining to the intervening molecular cloud.

a) Stellar Observations

i) *Optical Imaging*

Initial detection of the optical counterpart of H0253+193 was performed on 1987 January 28 using our CCD-based imaging polarimeter. We obtained 5 minute direct images in I band (9000 Å) of the 5′ × 5′ field centered on the X-ray position determined by HP; $\alpha(1950) = 2^h53^m20^s.5$, $\delta(1950) = +19°14'38''$. Because of partially overcast sky conditions, no stellar objects appeared in the raw images, though postprocessing including flat-fielding did reveal the presence of one star. The following night, January 29, the sky was clear and the raw I-band frames clearly showed the same star. We also obtained 10 minute R and V images and a 20 minute image through a 75 Å wide filter centered at Hα. None but the I-band images showed the presence of the star or any other features (such as HH objects). Because there were no other stars in the I-band images, the position of the star was determined by offsetting the telescope from the nearest SAO star (SAO 093190) to be $\alpha(1950) = 2^h53^m22^s.3$, $\delta(1950) = +19°13'32''.4$. This position is about 26″ east and 66″ south of the X-ray position, for a total offset of 70″ (see insert Fig. 1). While this difference is over twice the size of the estimated positional uncertainty (32″; HP), there are no sources to at least 4–5 mag fainter at I which are closer to the X-ray position. In § V below, we detail all the evidence for the association of the I-band star with H0253+193.

Figure 1 shows a plan view of the region around the X-ray source H0253+193. The figure shows a 2° × 2° region of sky, with the visible SAO stars indicated as filled circles. The expanded box shows the 5′ × 5′ field imaged at V, R, Hα, and I bands. The HP X-ray position and error box are shown, as is the position of the I-band star we found.

The I-band magnitude of the star was about 17.3 ± 0.5 and was obtained relative to observations of standard stars in the globular cluster NGC 2419 (Christian *et al.* 1985). The lack of a detection of the star in the R-band frame to a limiting magnitude of about $m_R = 19.5$, indicated a minimum $(R-I)$ color of at least 2 mag, confirming the very red nature of this star. Since an embedded star would be expected to suffer significant reddening from the intervening cloud material, the star was positively identified as being within or behind the cloud. No HH objects were seen in the 5′ frame to a limiting integrated flux across the Hα filter of 1.2×10^{-14} ergs s^{-1} cm^{-2}.

We reobserved the star on 1987 September 27 using the 1.5 m telescope and the imaging polarimeter instrument, but without the reducing optics and polaroid analyzers, giving an effective plate scale of 0.″3 per pixel with no light being lost due to the polaroid. During these observations we attempted to search for temporal variations in the brightness of the star at I band. Our procedure consisted of obtaining short, 1 s, I-band images of each of the three nearest SAO stars which surround the I-band star (SAO 93190, 93217, and 93155; see Fig. 1) followed by a 5 or 6 minute image of the field toward H0253+193. The SAO star observations were then fitted to obtain atmospheric extinction values and the extrapolated count rates for the stars outside the atmosphere. These values were used to normalize the individual SAO star observations and were averaged over the three stars to create normalization

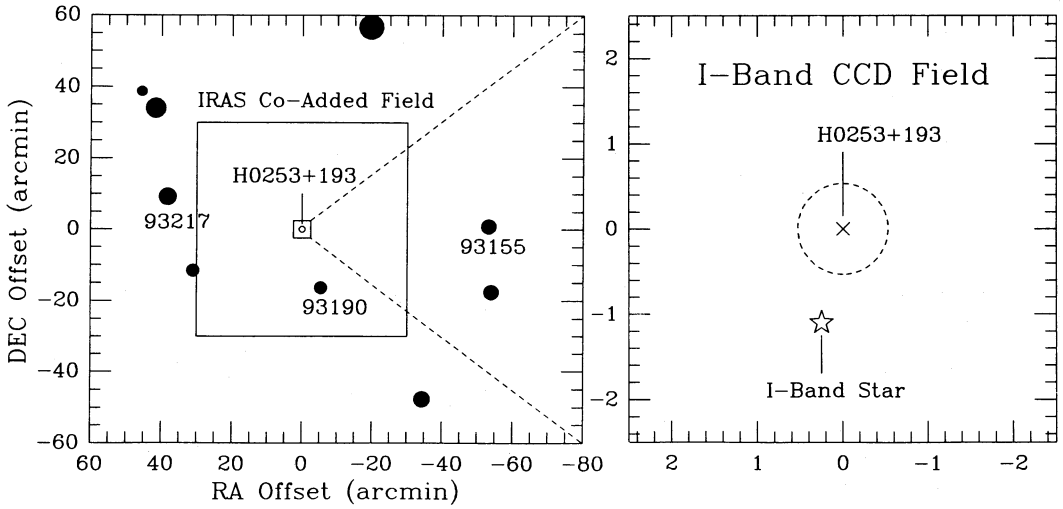

FIG. 1.—Plan view of 2° × 2° region around the position of H0253+193. All stars brighter than $m_v = 9.2$ are shown. The three SAO stars used to normalize the I-band time-resolved photometry are indicated by their SAO numbers. The region of the 1° × 1° *IRAS* field which was co-added and analyzed is indicated as a large box. The insert shows a blow-up of the central 5′ × 5′ which was deep imaged to search for the optical counterpart. The nominal X-ray position and error circle are indicated, as is the location of the I-band star found. The next brightest star in the CCD field is 4 mag fainter than this 17.5 mag object.

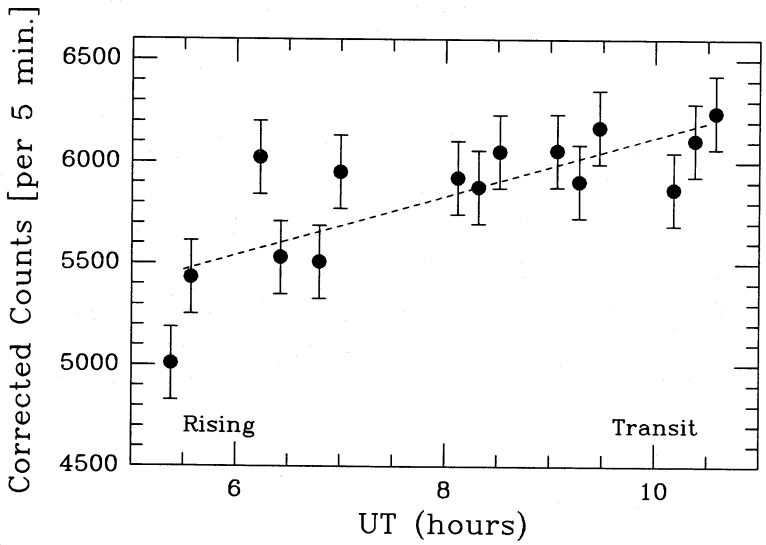

FIG. 2.—Plot of the corrected count rate of the *I*-band star vs. UT for 1987 September 27. Each observation of the star represents a single 5 or 6 minute *I*-band CCD integration, suitably corrected by two sets of observations of each of the three SAO star indicated in Fig. 1. The slope of the best-fit line is 0.028 ± 0.005 mag per hour. The times when the *I*-band star was at 2 air masses and at 1.03 air masses are indicated as "Rising" and "Transit," respectively.

factors for the *I*-band star observations. The observations of the *I*-band star, suitably normalized in this fashion, span almost 6 hr of time with 15 separate observations of the star. Figure 2 shows the run of corrected counts for the star versus Universal Time. The slope of the counts with time indicates a change in brightness of 0.028 ± 0.005 mag per hour. This is possible evidence for temporal variation of the star, though another explanation is possible (see § VII).

During the September observing, we also obtained a deep 15 minute *R*-band image. This image did show detectable emission from the star. Concurrent observations of the stars in NGC 7006 at *R* and *I* band were reduced using the recent measurements of their magnitudes by L. Davis (private communication) for her extension of the Christian *et al.* work. The derived *I*-band brightness for the star was found to be 17.60 ± 0.06 and the $(R-I)$ color was found to be +2.94 ± 0.30 after transforming to the Landolt (1983) system. The uncertainties contain contributions from readout noise, stellar photon noise, and uncertainties in the color transformations and extinction coefficients.

A final set of direct images was obtained on 1987 December 21 using the imaging polarimeter on the 90 inch (2.3 m) Steward Observatory telescope on Kitt Peak. Observations of NGC 7790 were obtained in *B*, *V*, *R*, and *I* bands both before and directly after observations of the star at *I* and *V* bands. The NGC 7790 stars were also reduced to the Landolt system using magnitudes provided by Davis. The *I*-band magnitude obtained for H0253+193 was slightly less, $m_I = 17.40 \pm 0.06$, than that seen 2 months earlier. The star was also detected in each of two 20 minute *V*-band frames. The derived $(V-I)$ color was +5.59 ± 0.82, where the uncertainty is almost entirely due to the magnitude variation between the two faint *V*-band detections.

ii) *Optical Spectroscopy*

During 1987 November 19–21, we used the Boller & Chivens spectrograph of the 2.3 m telescope and a thinned, UV-flooded TI 800 × 800 CCD (Carone *et al.* 1987) to obtain red, long-slit spectra of the *I*-band star. Because the acquisition TV, which views light reflected off the silvered spectrograph slit jaws, is blue-sensitive, we acquired the star by offsetting from SAO 93190. The 2″.5 × 4′ wide slit was oriented with its long direction in right ascension to reduce the effects of short-term tracking errors. The *I*-band star was centered by taking a set of short spectra (5 minute) at positions separated by about 2″ in declination. We integrated the light seen in the spectra and returned to the declination corresponding to maximum light through the spectrograph. A suitable guide star was found in the field of the offset guider and all subsequent spectra were obtained while manually guiding.

During the first night, a grating with 300 lines per millimeter was used to cover the wavelength range from just blueward of Hα, 6300 Å, to 9300 Å at 3.73 Å per pixel. During the second night a grating with 570 lines per millimeter was used to cover 8200 to 9800 Å at 2.03 Å per pixel. The wavelength scale was derived from observations of a He-Ne arc lamp and the spectra were flat-fielded using a continuum lamp. The spectra for the *I*-band star were extracted from the long-slit data using IRAF.[1] Incomplete subtraction of the very strong OH bands in the spectrum and fringing due to the thinness of the CCD chip remain in the final spectrum.

The sum of 12 individual 20 minute spectra from the first night is presented in Figure 3. The deep absorption seen near 7600 Å is due to telluric oxygen, and the emission feature near 8800 Å is due to telluric OH. The remaining features between 8300 Å and the end of the spectrum are due to telluric OH and fringing. Note that Hα is not seen, either in emission (as would be typical of a T Tauri star) or in absorption. The limiting equivalent width is 4 Å. Also note that there are essentially no stellar absorption bands in this spectrum. The higher dispersion spectra from the second night similarly show no stellar features.

In § III, below, we show how this spectrum, with its lack of stellar features, can be used to obtain the spectral type of this star.

[1] IRAF is distributed by National Optical Astronomy Observatories, which is operated by the Association of Universities for Research in Astronomy, Inc., under contract to the National Science Foundation.

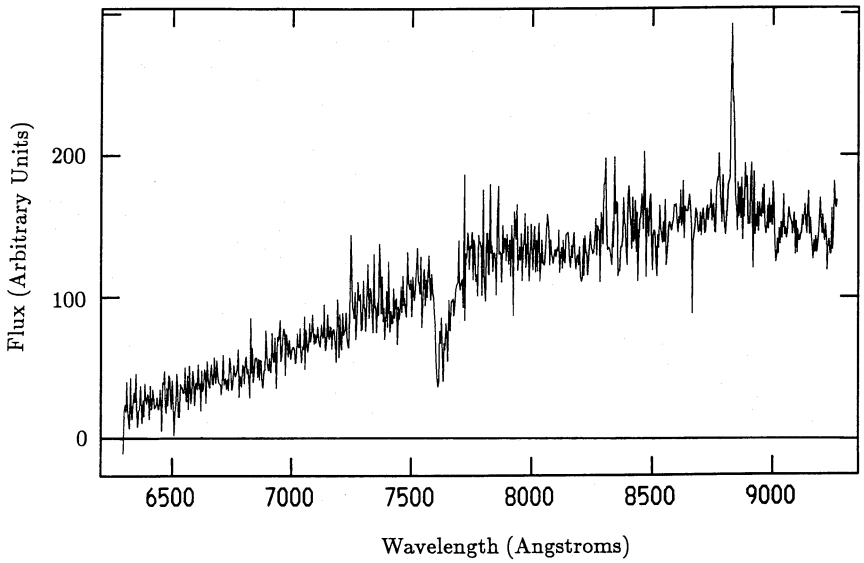

FIG. 3.—Optical spectrum obtained on the 2.3 m telescope 1987 December 19. This spectrum is only partially flux-corrected, so the flattening beyond 8000 Å is not real. This spectrum is a sum of 12 individual 20 minute spectra. The slit size was 2".5 along the declination direction and 4' along the right ascension direction. The features at 7600 and 8800 Å are due to telluric oxygen and OH. The wiggles beyond 8800 Å are due to interference (fringing) in the thin TI chip. There is no emission or absorption at Hα (to 4 Å EW) or any other wavelength due to the star.

iii) *Optical Polarimetry*

During the initial 1987 January observing run on the 1.5 m we also obtained, on January 30, *I*-band polarimetric images of the star using the imaging polarimeter with HN-7 as the analyzing polaroid. Four 5 minute images were obtained, one each through the polaroid at relative orientation angles of 0°, 45°, 90°, and 135°. These images were flat-fielded using observations of the interior of the dome similarly obtained through the same polaroid orientations. Stokes *U*, *Q*, and *I* were formed from the integrated count rates measured for the star in the four images. The derived polarization for the star was 8.1%. The two intensities (I_{0+90} and I_{45+135}) were found to differ by 1.8%, and this value is a good estimate of the uncertainty of the polarization (the photon noise is estimated at about 1.5%). Since polarization is a positive definite quantity, and the uncertainty for this measurement is fairly high, the most likely polarization is somewhat lower, $P = 7.9\%$ (Wardle and Kronberg 1974), and even lower if the uncertainty is underestimated.

This moderate value of the polarization is indicative of the polarization induced by an intervening molecular cloud on the light from background stars (Vrba, Strom, and Strom 1976) and not of the higher polarization values (20%–40%) produced by scattering of light off dust contained in an embedded reflection nebulae. Hence it is likely that the *I*-band light is from the photosphere of the star and not from some larger dust shell.

iv) *Near-Infrared Imaging*

On 1987 September 6–7, we used the Rieke near-infrared 64 × 64 pixel CCD camera (Rieke *et al.* 1988) with a 1'.1 × 1'.1 field of view on the 1.5 m telescope to observe the *I*-band star. The star was easily detected in the *J*, *H*, and *K* bands and through a narrow-band filter centered at the wavelength of the CO band head near 2.35 μm. These observations were transformed to the system of Elias *et al.* (1982) through observations of four of their faint standard stars in 1988 April, also on the 1.5 m telescope (see Appendix). In Table 1 we present a summary of the near-IR and optical photometric observations. All of the observations have been corrected for atmospheric extinction but have not been corrected for reddening (see § III).

b) Cloud Observations

i) *IRAS Co-Added Images*

Co-added *IRAS* data for the 1° × 1° field centered near our detected star were obtained and partially analyzed at the Image Processing and Analysis Center (IPAC) in Pasadena, California. These images are significantly more sensitive to weak emission from cold dust than either the *IRAS* Point Source Catalog or *IRAS* sky flux images. The 100 and 60 μm images were registered and combined to form images of the derived dust temperature $T_{60/100}$ and 100 μm dust opacity τ_{100} (here assuming a λ^{-1} emissivity law). Figure 4 shows the dust opacity map for the L1457 cloud core. The size of the cloud is about 30', which at a distance of 65 parsecs indicates a physical size of about a half a parsec. This size is virtually identical to the average size of the Bok globules in the catalog of Clemens and Barvainis (1988). Further, the size of the region showing the highest dust opacity in the center of the cloud is barely resolved at about 5' or 0.1 pc in size. This size is similar to the sizes of the dark cloud cores studied by Myers, Linke, and Benson (1983). The maximum dust opacity occurs about 1'.7 north of the *I*-band star position and has a value of 0.000141. At the position of the star the opacity has a value of 0.000082, about half the value of the peak opacity. The derived $T_{60/100}$ dust temperature is 26 K in the cloud core and somewhat

TABLE 1

LOG OF OBSERVATIONS

Filter	1987 Jan 28 (1.5 m)	1987 Sep 6–7 (1.5 m)	1987 Sep 27 (1.5 m)	1987 Dec 21 (2.3 m)
V	>20	...	...	23.00 ± 0.82
R	>19.5	...	20.54 ± 0.30	...
Hα	>17.6	...	...	...
I	17.3 ± 0.5	...	17.60 ± 0.06	17.40 ± 0.06
J	...	13.54 ± 0.15	...	...
H	...	12.24 ± 0.15	...	...
K	...	11.61 ± 0.15	...	...
[CO]	...	−0.079 ± 0.020	...	...

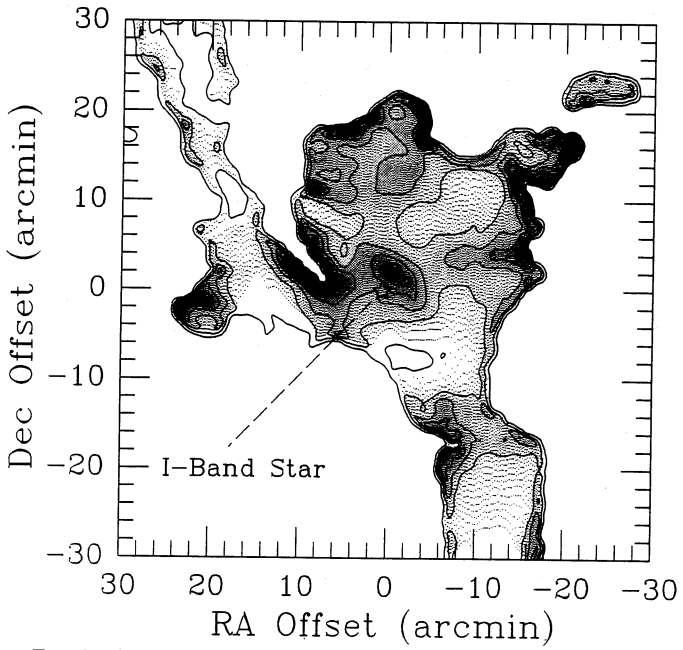

FIG. 4.—Contour representation of the dust opacity toward the L1457 cloud core, as seen by *IRAS*. This plot was computed from the 100 and 60 μm emission maps produced by co-adding all the satellite passes across this region. The spatial resolution is about 2′–3′. The lowest contour corresponds to $\tau_{100} = 8 \times 10^{-6}$ and subsequent contours are spaced by optical depth values of 2.4×10^{-5}. The outer edges of the cloud indicate a size of roughly 30′ or 0.5 pc. The highest opacity region has a size of about 5′ or 0.1 pc, similar to the size of other dark cloud cores. The corresponding temperature map shows a central temperature of 26 K, with edge temperatures somewhat higher than 30 K. The line of sight to H0253+193 passes only about 1.′7 south of the center of the cloud (indicated by a star on the figure).

higher (30–35 K) in the outer regions of the cloud, similar to the behavior seen in other cloud cores (Heyer *et al.* 1988; B5—Beichman *et al.* 1988). In the 25 and 12 μm co-added maps, no point or extended sources appear near either the *I*-band star or the high dust opacity core. Instead, both maps show faint *absorption* of the background emission at the location of the high opacity core. Thus there are no embedded objects which are heating the cloud dust enough to emit at 12 or 25 μm. This places a rather strong constraint on the maximum IR luminosity of any embedded object.

ii) CO *Millimeter-Wave Spectroscopy*

During 1988 March 11 through 22, observations of the $J = 2$–1 spectral lines of ^{12}CO (hereafter CO), ^{13}CO, and C^{18}O near 1.3 mm were obtained using the Millimeter-Wave Observatory[2] at Mount Locke near Fort Davis, Texas. A total of 13 positions (1′ spacings and beam size) within 2′ of the position of the detected star were observed at the CO wavelength, 11 positions at ^{13}CO, and only one position, directly toward the detected star, at the C^{18}O wavelength. All observations were obtained using a 250 kHz filter bank (velocity resolution $\sim$0.34 km s^{-1}) in frequency-switched mode. The spectra were calibrated using a chopper wheel, and pointing and efficiencies were determined by continuum scanning across Jupiter and Venus. The main beam efficiency was found to be 0.66, and this value was used to correct the antenna temperatures of all the spectra. After removing standing waves induced by the frequency switching, the spectra were folded to rectify the lines and the baselines again fitted to remove curvature.

The lines of CO and ^{13}CO (uncorrected for efficiency) obtained toward the star position are shown in Figure 5. Although the stronger CO line shows a strong dip near velocity -3.5 km s^{-1} which is reminiscent of self-absorption, and which might be expected for the core of a quiescent Bok globule (Dickman and Clemens 1983), the ^{13}CO spectrum shows two distinct spectral lines. Hence the CO spectra for this cloud are composed of the lines resulting from two molecular components. One component (at a line center velocity of -5 km s^{-1}) has a warmer excitation temperature and has a larger column density of ^{13}CO; the other component (with a line center velocity of -2.5 km s^{-1}) has a cooler excitation temperature and has a smaller column density of ^{13}CO.

Analysis of the CO lines for the two components using all the spectra shows that the mean excitation temperature for the warmer component is 10.8 K and for the cooler component is 8.3 K. The line center ^{13}CO opacities are 0.66 for the warmer component and 0.35 for the cooler component, assuming ^{13}CO and CO have the same excitation temperature (LTE assumption). The mean LTE column density of ^{13}CO molecules is 4.3×10^{15} cm^{-2} for the warmer component and about one-fourth of that for the cooler component. Thus the total LTE column density through the molecular cloud along the direction to the *I*-band star is around 5.4×10^{15} ^{13}CO molecules cm^{-2}. Using a standard dark cloud conversion of this column density to optical extinction (Dickman 1978), a total LTE extinction through the cloud of 2.7 mag at *V* band is obtained.

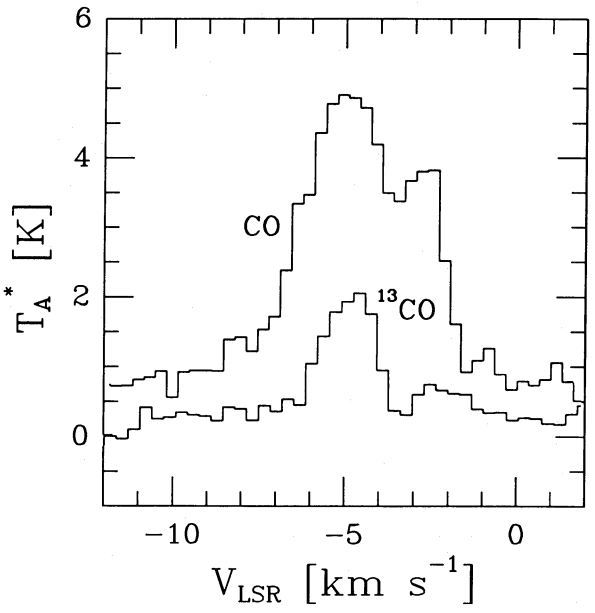

FIG. 5.—Millimeter CO and ^{13}CO spectra obtained at the MWO toward the direction of the *I*-band star. The spectra are offset from each other by 0.5 K of corrected antenna temperature. Note that *both* spectra are bifurcated into two overlapping spectral lines produced by a warm, dense component (at $V = -5$) and a cooler, thinner component (at $V = -2.5$).

[2] The Millimeter-Wave Observatory is operated by the Electrical Engineering Research Laboratory of the University of Texas at Austin with support from the National Science Foundation and McDonald Observatory.

This low value for the extinction indicates either that the ^{13}CO is very subthermally excited or that the abundance of CO molecules in this cloud is significantly less than in typical dark clouds. It is also possible that *both* of these effects are occurring in this cloud. Hence, the value of 2.7 mag represents a lower limit to the optical extinction for this cloud.

A crude upper limit to the CO-traced extinction can be obtained by assuming the ^{13}CO is subthermally excited and by estimating an appropriate excitation temperature. As the excitation temperatures for ^{13}CO are lowered from the ^{12}CO values, the inferred ^{13}CO column density increases for a fixed, observed ^{13}CO line profile. However, for excitation temperatures of the dominant line component below about 7 K, the inferred ^{13}CO opacity becomes infinite, indicating that trapping in the ^{13}CO line will assist in thermalizing the line. Hence realistic estimates of the ^{13}CO excitation temperature are in the range of 10.8 to about 8 K. At 8 K, the derived total A_V is 5 mag. Thus the molecular cloud L1457 contributes a minimum of 2.7 and a maximum of 5 mag to the total extinction at V band.

III. THE SPECTRAL TYPE OF THE STAR

There are two paths to identifying the spectral type of the I-band star. One method is to identify which spectral types show no lines (to the appropriate limits) in the passband of our optical spectrum. The second method uses the depth of the near-IR CO band head as an approximate indicator of spectral type (Jones, Hyland, and Bailey 1984).

For stars as late as mid-K to early-M, strong bands of TiO are present between 6569 and 8505 Å. Since our spectrum lacks these lines, the stellar type must be earlier than mid-K. Stars as late as F show strong lines of Hα which are also not present in our spectrum. Hence, from the lack of lines in our optical spectrum, we deduce a spectral type somewhere in the G to mid-K range. Note that G5 stars typically show Hα absorption of about 3 Å EW, somewhat below our limit of 4 Å EW.

For giants and dwarfs later than G0, the near-IR [CO] index is a good indicator of spectral type. In the presence of reddening, however, the observed index must be corrected. Indeed, our uncorrected [CO] value of -0.079 is significantly brighter than that seen in any star measured by Frogel *et al.* (1978) or Persson *et al.* (1983). Jones *et al.* used CVF observations of the CO band head and corrected for reddening using the slope of the spectra obtained outside the band head, expressed as excess $H-K$ color, $E(H-K)$. For our set of narrow and wide filters (centered at 2.35 and 2.22 μm, respectively), we determine a reddening correction using the extinction law of Rieke and Lebofsky (1985) as follows:

$$[CO]_{CORRECTED} = [CO] + 0.0084A_V \quad (1)$$

or, similar to Jones *et al.*,

$$[CO]_{CORRECTED} = [CO] + 0.133E(H-K)\,. \quad (2)$$

The intrinsic $(H-K)$ colors of giants and dwarfs between spectral types of G0 and K5 are between 0.04 and 0.15 (Frogel *et al.*; Johnson, MacArthur, and Mitchell 1968). If we adopt a mean $(H-K)$ color of 0.09, the excess is 0.535 mag and the corrected [CO] index is roughly zero. We show below that the extinction to the star, measured across both optical and near-IR wavelengths, may be somewhat higher than the value inferred from the $(H-K)$ color excess. Hence the corrected [CO] index should be increased above zero somewhat. Also, as the [CO] index approaches zero, the spectral type of the star becomes earlier and lowers the intrinsic $(H-K)$. That net effect is that the "best-fit" corrected [CO] index is about 0.02–0.03, and the inferred spectral type is roughly G5 (Frogel *et al.*) with an uncertainty of about one-half of a spectral type.

Unfortunately, the luminosity class of the star is harder to extract from the observations. Both G5 giants and dwarfs show a lack of strong optical lines in the range of our optical spectrum and, although they have different near-IR colors, the differences are much smaller than the uncertainties in the extinction and cannot be distinguished. The luminosity class indicator for G5 stars is the discontinuity near 4215 Å (Allen 1976). However, our star has an estimated blue magnitude fainter than 27th, making blue spectroscopy difficult.

IV. EXTINCTION THROUGH THE CLOUD

Possessing the spectral type of the I-band star and the observed colors from V through K bands, we can determine the extinction and the distance to the star (assuming various luminosity classes).

Table 2 lists the color excesses and Table 3 lists the dereddened magnitudes for the star. The reddening was determined from a best-fit line through the run of excess color with inverse wavelength. The extrapolated excess $(B-V)$ color so determined was 3.65 ± 0.46 mag. For a ratio of total to selective extinction of 3.1, the inferred V-band extinction is 11.3 ± 1.4 mag. This value was used to produce the dereddened magnitudes of Table 3 using the extinction law of Rieke and Lebofsky (1985).

From the dereddened V magnitude, the distance to the star can be estimated. Calculating a distance modulus for G5 stars of luminosity class from Ia to VI using Allen (1976), the farthest derived distance is 72 kpc for the Ia luminosity class G5 supergiant. The nearest distance is 120 pc for a Population II subdwarf. Unless the star is a Population II subdwarf which has somehow strayed into the cloud (a very unlikely source of strong X-rays), the star, for any normal luminosity class, cannot be inside the cloud. Benchmark distances are 200 pc for a dwarf and around 2 kpc for a giant.

TABLE 2

COLOR EXCESSES

Color	Excess (mag)
$(V-R)$	1.77
$(R-I)$	3.00
$(I-J)$	3.60
$(J-H)$	0.99
$(H-K)$	0.58

TABLE 3

DEREDDENED MAGNITUDES

Filter	Magnitude
V	11.70
R	12.09
I	12.05
J	10.35
H	10.26
K	10.33
[CO]	+0.02

V. IDENTIFICATION OF THE *I*-BAND STAR WITH H0253+193

We identify our *I*-band star with the X-ray source H0253+193 based on three criteria. These are (1) positional coincidence; (2) extinction coincidence; and (3) the ratio of X-ray to optical fluxes.

The measured positional offset of the *I*-band star from H0253+193 is 70″. HP list a 32″ radius error circle for the IPC detected X-ray object from a total of 114 counts. However, Maccacaro *et al.* (1982), similarly using the *Einstein* IPC, quote a 60″ radius uncertainty value for their Medium Sensitivity Survey (MSS). The next nearest *I*-band source is some 2.′5 away from the X-ray position and no sources brighter than $m_I = 21.7$ mag are closer than our *I*-band star. Hence, although our star is outside the formal error circle, we believe that the positional agreement is good.

The derived extinction to the *I*-band star, $A_V = 11.3 \pm 1.4$ mag, is also similar to the low end of the extinction range derived from the X-ray spectrum, 10 mag $< A_V <$ 75 mag, by HP. While this does not necessarily associate the *I*-band star with the X-ray source, it does place both objects *beyond* the molecular cloud (whose LTE CO-traced opacity is 2.7 mag).

Placement of the optical and X-ray source(s) beyond the distance to the cloud L1547 puts severe restrictions on the nature of the X-ray source. For example, the derived X-ray luminosity, assuming a minimum distance of 65 pc to the cloud, is $\log (L_X) \sim 31$ ergs s^{-1}, which far exceeds the range of X-ray luminosities seen for quiescent dwarf G and K stars [$\langle \log (L_X) \rangle_{dG} \sim 27.4$ ergs s^{-1}], and barely overlaps the dM star range (Maggio *et al.* 1987). Our optical spectrum eliminates the dM possibility, because of the lack of TiO bands seen.

Further, if we assume that the X-ray and *I*-band sources are *not* associated, we can compute a minimum ratio of X-ray to optical flux. For our *I*-band limit of 21.7 mag and assuming a similar $(V-I)$ color of 5.7 mag for any undetected optical source (due to the cloud extinction), the minimum flux ratio is: $\log (F_X/F_V) > 1.9$. However, Stocke *et al.* (1983) studied the nature of the X-ray sources seen in the MSS and show in their Figure 3 how the sources are distributed in V magnitude versus X-ray to V-band flux ratio. There are no objects in their figure with X-ray and optical properties anywhere near to those of our hypothetical nonassociation [$m_V > 16$, $\log (F_X/F_V) > 1.9$].

On the other hand, for the assumption of association between H0253+193 and our *I*-band star, the corresponding point on Figure 3 of Stocke *et al.* at [$m_V = 11.7$, $\log (F_X/F_V) = -1.5$] is within the region delineated by the stars Stocke *et al.* found to have detectable X-rays. Also, the location of our star on that figure rules out an extragalactic origin for the X-rays. The characteristics of the association also fit well on Figure 4 of the Stocke *et al.* paper, which shows how the X-ray to optical flux ratio varies with spectral class for their detected stars. Our object occupies the X-ray bright region of the G5 stars.

Hence, the identification of our *I*-band star as the optical counterpart of H0253+193 is based on the positional agreement, extinction similarity, and the limits imposed by the ratios of X-ray to optical fluxes for nonassociation versus association. The X-ray bright nature of the source can be understood as possibly originating from a RS CVn system.

VI. H0253+193 AS A RS CVn SYSTEM

Silva *et al.* (1985) and Bergoffen *et al.* (1988) examined the nature of the stellar objects showing X-ray emission which have the largest ratio of X-ray to optical flux for a given spectral type. In both studies, rather than finding normal, quiescent late-type stars, a high fraction of RS CVn systems were found.

The optical properties of RS CVn stars are reviewed by Hall (1981), Catalano (1983), Charles (1983), and Bopp (1983) and the X-ray properties have been studied by Walter and Bowyer (1981) and Majer *et al.* (1986). RS CVn systems consist of close binaries of late spectral type with dwarf to giant luminosities. Although mass transfer is not particularly important, these binaries exhibit starspots and coronal loops which may connect the two stars. It is the interaction of (and possible connection between) the stars which drives the X-ray emission to exceed that of normal stars of the same spectral class. In unbiased X-ray sky surveys, the stellar systems found tend to be dominated by pre–main-sequence stars (such as T Tauri stars) and RS CVn systems (Stern *et al.* 1981; Helfand and Caillault 1982; Silva *et al.* 1985; Bergoffen *et al.* 1988). Hence, it is reasonable to examine H0253+193 for RS CVn characteristics, once its T Tauri characteristics are found to be absent.

If H0253+193 is a RS CVn binary system, then several of its observed properties can be more easily understood. In particular, the X-ray spectral temperature, ratio of X-ray to optical flux, X-ray luminosity, and optical colors (see § VII) are all easily explained by the RS CVn interpretation.

HP fitted the observed X-ray spectrum to obtain $kT > 4$ keV [$\log (T) > 7.7$] and 10 mag $< A_V <$ 75 mag. Our measured extinction to the star, 11.3 mag, can be combined with the curves shown by HP in their Figure 2, to obtain a best-fit X-ray spectral temperature of 11 keV [$\log (T) = 8.1$]. While this temperature exceeds those normally seen in RS CVn systems (Majer *et al.*), it may be entirely reasonable. Majer *et al.* separated their sample of RS CVn systems into nearby (distance ≤ 90 pc) and distant groups. They found that the nearby binaries often required a two-temperature fit to explain the observed X-ray spectra, while for the distant systems, single-temperature fits were the norm. The two temperature fits of the nearby RS CVn systems [with typically $\log (T_{LOW}) \sim 6.5$ and $\log (T_{HIGH}) \sim 7.25$] closely resemble those found for the X-ray spectra of normal late-type dwarf stars (but the RS CVn systems have much higher luminosities). The distant RS CVn systems exhibited X-ray temperatures similar to the values of T_{HIGH} fitted for the nearby RS CVn systems. The interpretation favored by Majer *et al.* is that RS CVn systems exhibit a broad range of coronal temperatures, fairly well approximated by a two-temperature model. However, even modest amounts of extinction strongly suppress the lower temperature contributions, allowing a single fit with a T_{HIGH} value, which itself has been somewhat elevated due to extinction.

For H0253+193, which has a relatively huge extinction compared with the RS CVn systems studied to date, we expect the spectrum to shift even farther to the higher energies. Hence the value of $\log (T)$ obtained, about 8.1, though above the range seen for lower extinction RS CVn systems, may be entirely appropriate for this highly extincted system.

The ratio of X-ray to optical flux is easily understood in the context of a RS CVn interpretation, also. Our dereddened ratio of $\log (F_X/F_V) = -1.5$ (or somewhat less, ~ -2; see § VII) is higher than the highest seen in the MSS for quiescent G5 spectral class stars (Stocke *et al.* 1983). However, from the surveys of Silva *et al.* (1985) and Bergoffen *et al.* (1988), discussed above, one might *predict* that H0253+193 should be a RS CVn system, because of the high ratio.

The X-ray luminosity of H0253+193, estimated to be

$\sim 10^{31}$ ergs s^{-1} by HP, must be increased since the distance to the system has grown from 65 pc to between 200 and 1600 pc. For a single G5 subgiant dominating at V-band (see § VII), the photometric distance to H0253+193 is 500 pc. The luminosity at that distance, $L_X \sim 10^{32.8}$ ergs s^{-1}, is off the high end of the distribution of X-ray luminosities for the RS CVn sample of Walter and Bowyer (1981). If the luminosity class is lowered to that of the main sequence, L_X becomes 10^{32} ergs s^{-1}, which still makes H0253+193 somewhat more X-ray luminous than any RS CVn yet seen (Walter and Bowyer 1981; Majer *et al.* 1986).

In summary, by interpreting H0253+193 as a RS CVn binary system, several observational facts are explained. The high X-ray spectral temperature is partially a consequence of the large extinction to the system. The high value of the ratio of F_X/F_V is a *characteristic* of RS CVn systems and, at any fixed $(B-V)$, RS CVn systems exhibit the largest ratios. The X-ray luminosity of H0253+193 is at least 10^{32} ergs s^{-1} because the X-ray source is at least as far away as 200 pc. Together, these observations indicate that H0253+193 may be a RS CVn binary system with the highest X-ray luminosity and optical extinction (and possibly distance) yet observed.

VII. THE BINARY NATURE OF H0253+193

a) Period

Beginning with the conclusion that H0253+193 is a binary system, can we deduce any new information from the observations? Figure 2 shows how the I-band normalized count rate varies with time. Although the noise on the measurements is relatively large, the slope of the line fitted through the data points is significant. The value of the slope, 0.028 ± 0.005 mag per hour, can be divided into the expected range in magnitudes seen for RS CVn variables. These excursions are typically 0.1 to 0.3 mag at V (Hall 1981). A time scale for the observed variation would then be a little over three hours (unlikely, since we see only one variation) to about a day. This is the short period end of the range found by Walter and Bowyer (1981) for RS CVn systems. However, they found a relation between the ratio of X-ray to optical flux and period in the sense that systems with high values of this ratio (such as H0253+193) exhibited the shortest periods (around 1 day). Hence, our I-band photometry may have revealed an orbital period for H0253+193 close to 1 day.

Alternatively, the temporal variation in the count rate seen in Figure 2 could indicate that there is a significant color-correction term for the atmosphere in our I-band observations. The intrinsic colors of the SAO stars are all significantly bluer than the $(R-I)$ color of 3 mag for the I-band star. Thus the variation of the counts with UT could be explained as the variation of counts for an atmosphere which is more opaque for very red objects than for relatively blue objects. The atmospheric extinctions derived for the SAO stars have an average value of 0.109, while the I-band star (if *not* normalized using the SAO stars) has a derived extinction of 0.19. In Figure 2, the I-band star is rising from 2 air masses at 5 hr UT and transitting at 10 hr UT; hence the lower count rate at the earlier time could reflect the larger opacity in the far red. However, to confuse this issue, the two SAO stars with known spectral types (93190 and 93217) show the opposite effect. That is, the redder SAO star (93217-K type) shows the smaller atmospheric opacity relative to the bluer SAO star (93190-A9 V). The resolution may lie in the *extreme* redness of the I-band star, though.

b) Energy Distribution

In Figure 6, we show the dereddened photometric energies [log (λF_λ)] versus wavelength, assuming $A_V = 11.3$ mag and the extinction curve of Rieke and Lebofsky (1985). There are two points to notice regarding this figure. The first is that there is a bump near J which is very narrow. Second, the spectrum of these broad-band energies is too wide to be well-fitted by a single star. As RS CVn systems are binaries, we experimented with various combinations of stellar types and luminosity classes to try to synthesize the energy distribution of Figure 6.

In order to obtain this wide spectrum, two stars with very different colors were needed. A combination of G0 and M5 stars gives such a wide composite spectrum. However, to obtain energies similar to those observed across the entire wavelength range shown, the M5 star must have a much larger radius to make up for its cooler color. Shown on Figure 6 are the composite spectra obtained for two model systems. One system has a G0 V + M5 III pair and the other has a more luminous G star (G0 IV + M5 III). The giant nature of the M star in both systems is required to obtain the bright near-IR energies relative to the dwarf or subgiant G star. From the figure it seems that some combination of the models would yield an adequate description of the energy distribution; hence we favor a binary with stars similar to G0 V–IV + M5 III. Note, however, that M giants are rarely (if ever) found in RS CVn systems (e.g., Hall 1981).

We also tried changing the extinction to 10.3 and 12.3 mag. This is a reasonable parameter to vary since the assumption of a single G5 star, used to derive the extinction in § III, is violated somewhat by the binary nature of the system. These modifications did not produce spectra which were significantly better fitted by any of our combinations of spectral types and luminosity classes. An assessment of the quality of the matching (based on models including stars from G0 to M8) is that the spectral types are probably good to about one spectral type, the luminosity classes to about half a class, and the extinction to about half a magnitude (somewhat smaller than the 1.4 mag quoted above).

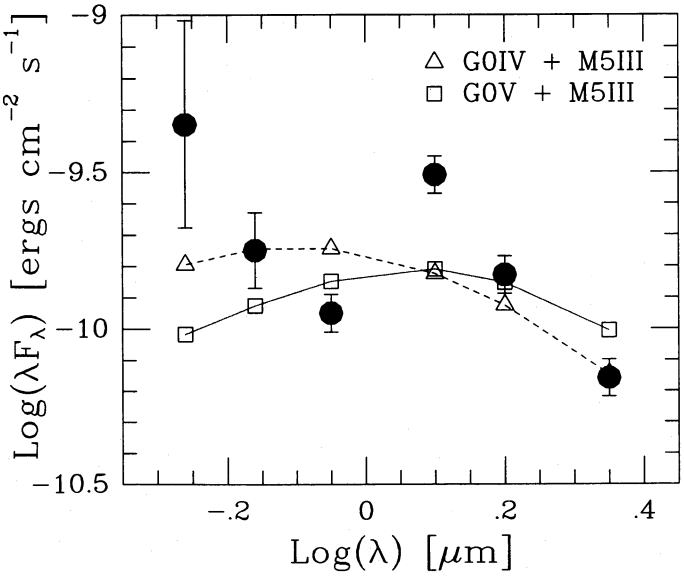

FIG. 6.—Dereddened energy distribution measured from optical and near-IR photometric observations (*filled circles*) compared to model binary star systems. The filled circle near log $(\lambda) = 0.1$ is the J-band point, which shows excess emission relative to the other filters.

Both of the above models, as well as many others attempted, failed to fit either the V-band or J-band energies. The J-band bump is narrower than any blackbody and will be hard to fit by a combination of blackbodies. Also, the dominance of the later type giant star in the near-IR (the M5 star emits between 60% and 90% of the combined K-band energy) is not supported by our measured [CO] index. For a M5 giant, the [CO] index ought to be around 0.22 to 0.25 (Frogel *et al.* 1978), and even when diluted by the G star, should strongly exceed the 0.02 to 0.03 index measured.

The proper explanation of the J-bump, V-band excess, and [CO] index may lie with the RS CVn nature of this binary system. RS CVn systems exhibit photometric and color variations which are tied to the orbital period and arise from starspots (Hall 1981). In addition, systems with large X-ray luminosities ($> 10^{32-33}$ ergs s^{-1}) may have a large fraction of their surfaces involved in starspots and flares (Charles 1983). Hence, our observations, which are not contemporaneous, may be partially contaminated by flaring or periodic light-curve variations. If the V-band magnitude measured is actually higher than is typical of this system (though most starspots *decrease* the light intensity), the extreme value of the X-ray to optical flux ratio is lowered somewhat.

Nevertheless, the spectrum (Fig. 6) can be used to constrain the possible models for this system. First, binary stars of similar spectral type cannot reproduce the broad shape observed. Second, the requirement of dissimilar spectral types requires dissimilar luminosity classes for the stars, in the sense that the cooler star is brighter. Hence, at least one star is a giant. Our experiments at spectrum matching further indicate that a G0 V–IV + M5 III pair can reproduce most of the observed properties of the energy distribution.

A more cautious alternative is to classify the system as a G5 star with an IR excess. This alternative may be the preferred one either if M giants in RS CVn systems are not allowed or if the IR emission is due to nonstellar material (a disk or shell, instead).

VIII. FUTURE WORK ON H0253+193

Our observations of H0253+193 have revealed the nature of this X-ray source to a large extent. However, there are several pieces of the puzzle left to be found.

First, and most important, the orbital period of the system must be refined. Our time-resolved I-band photometry merely indicates that a period around 1 day may be appropriate. The true period could be as long as a year or under a day. The faintness of the star, even at I-band, and its heavily reddened colors, seem to indicate that near-IR (2 μm) monitoring will be required to obtain an accurate period.

Verifying the chromospheric activity of the optical star, via the Ca II H and K lines, will be very difficult because the estimated blue magnitude is at or beyond 27th. Our observations at Hα during two epochs have shown no emission or absorption, but higher resolution may be required, as will multiepoch observations.

Our photometric observations should be extended into the mid-IR. Although the *IRAS* co-added images showed no 12 μm sources in the vicinity of H0253+193, they lack the sensitivity of deep ground-based observations. Photometry at 3, 5, and 10 μm would help constrain the spectral types of the stars in the binary system.

IX. SUMMARY

We have used deep I-band CCD imaging to discover the optical counterpart of the hard X-ray source H0253+193, seen along the line of sight toward L1457 (MBM 12), the nearest molecular cloud. Follow-up photometry at V, R, Hα, J, H, K bands and in the CO band (2.35 μm), polarimetry and time-resolved photometry at I band, optical spectroscopy from 6300 to 9800 Å, *IRAS* co-added imagery, and millimeter-wave CO spectroscopy have been obtained and interpreted to yield a consistent picture of the X-ray system.

Our findings are summarized as follows.

1. The spectral type of the I-band star is roughly G5 ($\pm$ half a spectral type), estimated from both optical spectroscopy and near-IR [CO] index photometry.

2. The extinction to the I-band star is 11.3 ± 1.4 mag at V-band.

3. The distance to the I-band star is at least 200 pc, and more likely equal to or in excess of 500 pc.

4. Hence, the I-band star is *behind* the molecular cloud and *not* associated with the cloud. The millimeter CO and *IRAS* traced column densities through the cloud lead to extinctions which are smaller than the near-IR and optically traced extinctions. These data yield a consistent conclusion of non-association between the star and the cloud.

5. The I-band star is the optical counterpart of the X-ray source H0253+193 based on positional agreement, extinction agreement, and the limits imposed by the inferred X-ray properties.

6. The optical spectrum shows no Hα to a limit of 4 Å EW. Deep Hα imaging of a $5' \times 5'$ region around H0253+193 reveals no HH objects to a limit of 1.2×10^{-14} ergs s^{-1} cm^{-2}.

7. The lack of Hα, location beyond the cloud, high ratio of X-ray to optical flux, and high X-ray luminosity argue against a T Tauri interpretation for the star.

8. We believe that the H0253+193 X-ray source may be a RS CVn binary system. As such, several observational facts are explained, such as the high X-ray spectral temperature [$\log (T) \sim 8.1$], the high X-ray luminosity [$\log (L_X) > 32$ ergs s^{-1}], the high X-ray to optical flux ratio [$\log (F_X/F_V) = -1.5$], and the width of the broad-band optical-IR energy distribution.

9. Experiments aimed at recovering the energy distribution all seem to require two stars of very different spectral types and luminosity classes to be present in the RS CVn binary. One such possible pair of stars, which does a fair job of reproducing the energy spectrum, is G0 V–IV + M5 III. However, problems remain in both the J and V bands. Alternatively, the spectrum may be classified as G5 + IR excess, as might arise from circumstellar material in shell or disk form.

10. A rough period near 1 day may be indicated from the time-resolved I-band photometry, the ratio of X-ray to optical flux, and the RS CVn interpretation. However, near-IR (2 μm) monitoring of this system is needed to refine the period.

Note added in manuscript.—As this paper was being revised, new X-ray results for H0253+193 were reported by Takano *et al.* (1989), who used the *Ginga* satellite during 1987 July 29 and 1989 January 23. Their discovery of X-ray pulses from H0253+193, with a period of 206 s, confirms the close binary nature of the stellar system we have studied. Further, as X-ray pulsations are associated with accretion, an inferred disk may be the source of the observed IR excess and could account for some of the optical extinction seen. Thus, the T Tauri explanation for H0253+193 has been independently ruled out by the new *Ginga* results.

We wish to thank Jim Treat for the near-IR CCD reductions which led to the transformations in the Appendix. Kim Dow provided manual guiding assistance during the optical spec-

troscopy. Lindsey Davis kindly supplied her photometry of NGC 7006 and NGC 7790 prior to publication. Marcia Rieke set up her IR CCD camera on the 1.5 m several times for us and provided much useful and cheerful help at understanding IR-CCD data analysis. Neal Evans chose to schedule us on the MWO during superb weather; we strongly thank him for his foresight. John Good and, especially, Gaylin Laughlin were extremely patient, calm, and helpful each time D. C. visited IPAC to process *IRAS* data and they helped make those visits very productive. Jules Halpern kept our interest level high and critiqued a draft version of this paper. Tom Bania shared his large-scale CO maps of the MBM 12 region prior to publication. This research has been partially supported by a Flinn Foundation grant of the Research Corporation, a NASA-*IRAS* GI contract, and by a grant from the Office of the Dean of the College of Liberal Arts at BU, all to D. C.

APPENDIX

COLOR TRANSFORMATIONS FOR THE RIEKE IR CAMERA

During 1988 April 24 to 29 we used the Rieke IR CCD camera on the 1.5 m telescope to calibrate the filters and camera response and to obtain the coefficients needed to transform onto the Elias *et al.* (1982) system.

We observed four stars from the list of faint standards (Table 2 in Elias *et al.*; HD 106965, HD 129655, Gl 299, and Gl 390). These stars were chosen chiefly to span the range of the [CO] index since we form the index differently than Elias *et al.* did. They used the differential counts detected between two, narrow filters, one centered on the CO band-head region and one just outside that region. We compare the counts seen in a narrow filter centered at CO to the wider K filter. Thus we needed to calibrate the relative widths of the filters.

The zero reddening transformations obtained are as follows:

$$K_{0,\mathrm{US}} = K_{\mathrm{Elias}} + (19.167 \pm 0.027) - (0.089 \pm 0.046)(J-K)_{\mathrm{Elias}}\,, \tag{A1}$$

$$(J-H)_{0,\mathrm{US}} = (0.97 \pm 0.10) + (0.881 \pm 0.043)(J-H)_{\mathrm{Elias}}\,, \tag{A2}$$

$$(J-K)_{0,\mathrm{US}} + (0.914 \pm 0.046) + (0.947 \pm 0.027)(J-K)_{\mathrm{Elias}}\,, \tag{A3}$$

$$(H-K)_{0,\mathrm{US}} = (0.022 \pm 0.032) + (0.885 \pm 0.161)(H-K)_{\mathrm{Elias}}\,, \tag{A4}$$

$$(CO-K)_{0,\mathrm{US}} = (2.114 \pm 0.017) + (4.403 \pm 0.648)[CO]_{\mathrm{Elias}}\,, \tag{A5}$$

where the K-band zero point assumes a 30 s exposure. Note that the slope of the CO transformation, 4.4, is related to the relative widths of the narrow CO and wide K filters we used.

The [CO] index transformation assumes no extinction. See equation (1) or (2) in the text for the reddening correction to obtain the intrinsic [CO] index.

REFERENCES

Allen, C. W. 1976, *Astrophysical Quantities* (London: Athlone).
Beichman, C. A., Wilson, R. W., Langer, W. D., and Goldsmith, P. F. 1988, *Ap. J. (Letters)*, **332**, L81.
Bergoffen, M. J., Stocke, J., Walter, F., and Fleming, T. A. 1988, *Pub. A.S.P.*, **100**, 736.
Bopp, B. W. 1983, in *Activity in Red-Dwarf Stars*, ed. P. B. Byrne and M. Rodono (Dordrecht: Reidel), p. 363.
Carone, T. E., Morris, S. L., and Leach, R. W. 1987, *Opt. Engineering*, **26**, 1043.
Catalano, S. 1983, in *Activity in Red-Dwarf Stars*, ed. P. B. Byrne and M. Rodono (Dordrecht: Reidel), p. 343.
Charles, P. A. 1983, in *Activity in Red-Dwarf Stars*, ed. P. B. Byrne and M. Rodono (Dordrecht: Reidel), p. 415.
Christian, C., Adams, M., Barnes, J. V., Butcher, H., Hayes, D. S., Mould, J. R., and Siegel, M. 1985, *Pub. A.S.P.*, **97**, 363.
Clemens, D. P., and Barvainis, R. 1988, *Ap. J. Suppl.*, **68**, 257.
Clemens, D. P., and Leach, R. W. 1987, *Opt. Engineering*, **26**, 923.
Dickman, R. L. 1978, *Ap. J. Suppl.*, **37**, 407.
Dickman, R. L., and Clemens, D. P. 1983, *Ap. J.*, **271**, 143.
Elias, J. H. 1978, *Ap. J.*, **223**, 859.
Elias, J. H., Frogel, J. A., Matthews, K., and Neugebauer, G. 1982, *A.J.*, **87**, 1029.
Frogel, J. A., Persson, S. E., Aaronson, M., and Matthews, K. 1978, *Ap. J.*, **220**, 75.
Hall, D. S. 1981, in *Solar Phenomena in Stars and Stellar Systems*, ed. R. M. Bonnet and A. K. Dupree (Dordrecht: Reidel), p. 431.
Halpern, J. P., and Patterson, J. 1987, *Ap. J. (Letters)*, **312**, L31 (HP).
Helfand, D. J., and Caillault, J.-P. 1982, *Ap. J.*, **253**, 760.
Heyer, M. H., Morgan, J., Snell, R. L., and Schloerb, F. P. 1988, preprint.
Hobbs, L. M., Blitz, L., Penprase, B., Magnani, L., and Welty, D. E. 1988, *Ap. J.*, **327**, 356.
Hobbs, L. M., Blitz, L., and Magnani, L. 1986, *Ap. J. (Letters)*, **306**, L109.
Johnson, H. L., MacArthur, J. W., and Mitchell, R. I. 1968, *Ap. J.*, **152**, 465.
Jones, T. J., Hyland, A. R., and Bailey, J. 1984, *Ap. J.*, **282**, 675.
Landolt, A. U. 1983, *A.J.*, **88**, 439.
Maccacaro, T., *et al.* 1982, *Ap. J.*, **253**, 504.
Maggio, A., Sciortino, S., Vaiana, G. S., Majer, P., Bookbinder, J., Golub, L., Harnden, F. R., Jr., and Rosner, R. 1987, *Ap. J.*, **315**, 687.
Magnani, L., Blitz, L., and Mundy, L. 1985, *Ap. J.*, **295**, 402 (MBM).
Majer, P., Schmitt, J. H. M. M., Golub, L., Harnden, F. R., Jr., and Rosner, R. 1986, *Ap. J.*, **300**, 360.
Myers, P. C., Linke, R. A., and Benson, P. J. 1983, *Ap. J.*, **264**, 517.
Persson, S. E., Aaronson, M., Cohen, J. G., Frogel, J. A., and Matthews, K. 1983, *Ap. J.*, **266**, 105.
Rieke, G. H., and Lebofsky, M. J. 1985, *Ap. J.*, **288**, 618.
Rieke, M. J., Rieke, G. H., and Montgomery, E. F. 1988, in *Infrared Astronomy with Arrays*, ed. C. G. Wynn-Williams and E. E. Becklin (Manoa: University of Hawaii), p. 213.
Silva, D. R., Liebert, J., Stocke, J. T., and Aaronson, M. 1985, *Pub. A.S.P.*, **97**, 1096.
Stern, R. A., *et al.* 1981, *Ap. J. (Letters)*, **251**, L105.
Stocke, J. T., Liebert, J., Gioia, I., Griffiths, R. E., Maccacaro, T., Danziger, I. J., Kunth, D., and Lub, J. 1983, *Ap. J.*, **273**, 458.
Takano, S., *et al.* 1989, *IAU Cicrular, No.* 4745.
Vrba, F. J., Strom, S. E., and Strom, K. M. 1976, *A.J.*, **81**, 958.
Walter, F. M., Brown, A., Mathieu, R. D., Myers, P. C., and Vrba, F. J. 1988, *A.J.*, **96**, 297.
Walter, F. M., and Bowyer, S. 1981, *Ap. J.*, **245**, 671.
Wardle, J. F. L., and Kronberg, P. P. 1974, *Ap. J.*, **194**, 249.

DAN P. CLEMENS: Department of Astronomy, Boston University, 725 Commonwealth Ave, Boston, MA 02215

ROBERT W. LEACH: Department of Astronomy, PA-210, San Diego State University, San Diego, CA 92182